PERGAMON

International Journal of Solids and Structures 39 (2002) 1241–1257

INTERNATIONAL JOURNAL OF SOLIDS and STRUCTURES

www.elsevier.com/locate/ijsolstr

Finite element solutions for plane strain mode I crack with strain gradient effects

S.H. Chen *, T.C. Wang

LNM, Institute of Mechanics, Chinese Academy of Sciences, Beijing 100080, China

Received 26 February 2001

Abstract

In this paper, a new phenomenological theory with strain gradient effects is proposed to account for the size dependence of plastic deformation at micro- and submicro-length scales. The theory fits within the framework of general couple stress theory and three rotational degrees of freedom ω_i are introduced in addition to the conventional three translational degrees of freedom u_i. ω_i is called micro-rotation and is the sum of material rotation plus the particles' relative rotation. While the new theory is used to analyze the crack tip field or the indentation problems, the stretch gradient is considered through a new hardening law. The key features of the theory are that the rotation gradient influences the material character through the interaction between the Cauchy stresses and the couple stresses; the term of stretch gradient is represented as an internal variable to increase the tangent modulus. In fact the present new strain gradient theory is the combination of the strain gradient theory proposed by Chen and Wang (Int. J. Plast., in press) and the hardening law given by Chen and Wang (Acta Mater. 48 (2000a) 3997). In this paper we focus on the finite element method to investigate material fracture for an elastic-power law hardening solid. With remotely imposed classical K fields, the full field solutions are obtained numerically. It is found that the size of the strain gradient dominance zone is characterized by the intrinsic material length l_1. Outside the strain gradient dominance zone, the computed stress field tends to be a classical plasticity field and then K field. The singularity of stresses ahead of the crack tip is higher than that of the classical field and tends to the square root singularity, which has important consequences for crack growth in materials by decohesion at the atomic scale.

Keywords: Strain gradient theory; Crack tip field; Finite element

1. Introduction

Recent experiments have shown that materials display strong size effects when the characteristic length scale is on the order of microns (Fleck et al., 1994; Stolken and Evans, 1998; Ma and Clarke, 1995; McElhaney et al., 1998; Nix, 1989; Poole et al., 1996; Lloyd, 1994). The conventional plasticity theory, however, cannot predict this size dependence because its constitutive model possesses no internal length scale.

* Corresponding author. Tel.: +86-10-6254-5533/2120; fax: +86-10-6256-1284.
E-mail address: chenshaohua72@hotmail.com (S.H. Chen).

0020-7683/02/$ - see front matter
PII: S0020-7683(01)00233-5

In 1994, Elssner et al. measured both the macroscopic fracture toughness and atomic work of separation of an interface between a single crystal of niobium and a sapphire single crystal. The macroscopic work of fracture was found to be two to three orders of magnitude higher than the atomic work of separation. This large difference between the macroscopic work of fracture and its counterpart at the atomic level was attributed to plastic dissipation in niobium, i.e., there must be significant plastic deformation associated with dislocation activities in niobium. However Elssner et al. (1994) observed that the interface between two materials remained atomistically sharp. Meanwhile the stress level needed to produce atomic decohesion of a lattice or a strong interface is typically on the order of 0.03 times the Young's modulus, or 10 times the tensile yield stress. But the maximum stress level that can be achieved near a crack tip is not larger than 4 or 5 times the tensile yield stress of metals, according to models based on conventional plasticity theories (Hutchinson, 1997). This clearly falls short of triggering the atomic decohesion observed in the experiments of Elssner et al. (1994). Attempts to link macroscopic cracking to atomistic fracture are frustrated by the inability of conventional plasticity theories to model stress–strain behavior adequately at the small scales involved in crack tip deformation.

In order to explain the size effect and the atomistically sharp crack tip in ductile niobium observed in the experiments of Elssner et al. (1994), it is necessary to develop a continuum theory for micro-level. Fleck and Hutchinson (1993) and Fleck et al. (1994) developed a phenomenological theory and a material length scale was introduced from the dimensional grounds. From these theoretical developments and consequent attempts at explaining experimental findings of indentation and fracture, it has been found necessary to introduce two length parameters (Fleck and Hutchinson, 1997). One length refers to rotational gradients as originally proposed in connection with the torsion measurements, the other scales with the stretch gradients. The latter is needed to rationalize length scale phenomena found in indentation and fracture. In 1998, Nix and Gao started from the Taylor relation and gave one kind of hardening law for gradient plasticity. Motivated by the hardening law, Gao et al. (1999) proposed a mechanism-based theory of strain gradient plasticity (MSG) based on a multiscale framework linking the micro-scale notion of statistically stored and geometrically necessary dislocations to the mesoscale notion of plastic strain and strain gradient. Huang et al. (2000a,b) used the MSG theory to analyze several problems successfully.

All the above strain gradient plasticity theories introduce the higher-order stress which is required for this class of strain gradient theories to satisfy the Clausiius–Duhem thermodynamic restrictions on the constitutive model for second deformation gradients (Gurtin, 1965a,b; Acharya and Shawki, 1995). In comparison, no work conjugate of strain gradient has been defined in the alternative gradient theories (Aifantis, 1984; Zbib and Aifantis, 1989; Muhlhaus and Aifantis, 1991) which represent the strain gradient effects in terms of the Laplacian of effective strain. Retaining the essential structure of conventional plasticity and obeying thermodynamic restrictions, Acharya and Bassani (1995) conclude that the only possible formulation is a flow theory with strain gradient effects represented as an internal variable, which acts to increase the current tangent-hardening modulus.

Shizawa and Zbib (1999) developed a thermodynamical theory of gradient elastoplasticity by introducing the concept of dislocation density tensor.

In 2000(a), Chen and Wang established a new hardening law based on the incremental version of conventional J_2-deformation theory, which allows the problem of incremental equilibrium equations to be stated without higher-order stress, higher-order strain rate nor extra boundary conditions.

As direct application, strain gradient plasticity theory has been used to investigate fracture of materials. Huang et al. (1995, 1997, 1999), Xia and Hutchinson (1996), Wei and Hutchinson (1997), Chen et al. (1998, 1999) and Chen and Wang (2000b, 2001) have investigated the asymptotic field near a crack tip as well as the full-field solution. It is established that, for the couple stress theory of strain gradient plasticity (Fleck and Hutchinson, 1993, Fleck et al., 1994, Chen and Wang, 2002), the stress level near a crack tip is not significantly increased as compared to that in classical plasticity. This is because the effect of stretch gradients, which is important near a crack tip, has not been accounted for. In order to incorporate this effect,

Chen et al. (1999) have used the theory of Fleck and Hutchinson (1997) to analyze the crack tip field. Indeed, stretch gradients can elevate the stress level near a crack tip, as also observed in steady-state crack propagation (Wei and Hutchinson, 1997). However, Chen et al. (1999) have shown that the asymptotic crack tip field in phenomenological strain gradient plasticity gives an incorrect, compressive stress traction ahead of a mode I crack tip. This is physically unacceptable since these compressive stress traction are clearly against our physical intuition, and are opposite to those in classical K field, HRR field, and the asymptotic crack tip field in the couple stress theory of strain gradient plasticity (Huang et al., 1995, 1997; Xia and Hutchinson, 1996; Chen and Wang, 2000b). Shi et al. (2000) investigated the structure of asymptotic crack tip fields associated with the developed theory of MSG plasticity and the result is the crack tip field in MSG plasticity does not have a separable form of solution.

In this paper, we investigate the plane strain mode I crack tip field using the new strain gradient theory, in which the rotation gradient and the stretch gradient are considered and couple stress that is work conjugate to the rotation gradient is introduced. The essential structure of the incremental version of conventional couple stress deformation theory is retained. Since the theory is in the incremental version, the asymptotic analysis is not convenient and finite element method is used to provide the near-tip stress and strain distributions for mode I crack tip field. The new strain gradient theory is given in Section 2. Numerical formulations with strain gradient effects are given in Section 3. Finite element results for crack tip fields in an elastic-power law hardening solid are shown in Section 4. Detail discussion is given in Section 5.

2. The new strain gradient theory

In fact, the present new strain gradient theory is the combination of the strain gradient theory proposed by Chen and Wang (in press) and the hardening law given by Chen and Wang (2000a). It preserves the essential structure of the incremental version of conventional couple stress deformation theory and no extra boundary value conditions beyond the conventional ones, are required. No higher-order stress or higher-order strain rates are introduced either. The key features of the new theory are that the rotation gradient influences the material character through the interaction between the Cauchy stresses and the couple stresses; the stretch gradient measures explicitly enter the constitutive relations only through the instantaneous tangent modulus and the boundary value problem of incremental equilibrium is the same as in the conventional theories. The tangent-hardening modulus is influenced by not only the generalized effective strain but also the effective stretch gradient.

2.1. Generalized strains

In a Cartesian reference frame x_i, the strain tensor ε_{ij} and the stretch gradient tensor $\eta^{(1)}_{ijk}$ (Smyshlyaev and Fleck, 1996) are related to the displacement u_i by

$$\varepsilon_{ij} = \tfrac{1}{2}(u_{i,j} + u_{j,i}) \tag{1}$$

and

$$\eta_{ijk} = u_{k,ij} \tag{2}$$

$$\eta'_{ijk} = \eta_{ijk} - \tfrac{1}{4}(\delta_{ik}\eta_{jpp} + \delta_{jk}\eta_{ipp}) \tag{3}$$

$$\eta^{s}_{ijk} = \tfrac{1}{3}(\eta'_{ijk} + \eta'_{jki} + \eta'_{kij}) \tag{4}$$

$$\eta^{(1)}_{ijk} = \eta^{s}_{ijk} - \tfrac{1}{5}(\delta_{ij}\eta^{s}_{kpp} + \delta_{jk}\eta^{s}_{ipp} + \delta_{ki}\eta^{s}_{jpp}) \tag{5}$$

The rotation gradient can be defined as the curvature tensor, which is related with the micro-rotation vectors ω_i,

$$\chi_{ij} = \omega_{i,j} \tag{6}$$

2.2. Effective rotation and stretch gradients

The effective strain is defined as

$$\varepsilon_e = \sqrt{\tfrac{2}{3}\varepsilon'_{ij}\varepsilon'_{ij}} \tag{7}$$

The effective rotation gradient χ_e is defined as

$$\chi_e = \sqrt{\tfrac{2}{3}\chi_{ij}\chi_{ij}} \tag{8}$$

The effective stretch gradient η_1 is

$$\eta_1 = \sqrt{\eta^{(1)}_{ijk}\eta^{(1)}_{ijk}} \tag{9}$$

2.3. Constitutive equations

There are a lot of works about couple stress theory, such as the works of Toupin (1962), Mindlin (1963, 1964), Schaefer (1967) and Eringen (1968). Specially, Green et al. (1968) proposed a dipolar theory of plasticity in the presence of simple force and stress dipoles. Also Naghdi and Srinivasa (1993, 1994) developed a Cosserat theory with three directors and solved problems involving the evolution of dislocations. All these theories are based on a reduced couple stress theory model, in which the micro-rotation vectors ω_i equals to the material rotation vector θ_i and $\boldsymbol{\theta} \equiv (1/2)\mathrm{curl}\,\boldsymbol{u}$. Then the relative rotation tensor α_{ij} vanishes, where α_{ij} is defined as $\alpha_{ij} = e_{ijk}\omega_k - (u_{j,i} - u_{i,j})/2 = e_{ijk}(\omega_k - \theta_k)$.

The new strain gradient deformation theory proposed here is based on the framework of general couple stress theory and is adapt to the real materials consisting of jillion discrete micro-particles (atoms, molecular or ions). The size of these particles is extremely small and about 0.3 nm. An idealized model for such kind of material is that the size of the particles is infinite small and the materials are full of these particles. Each particle has six degrees of freedom, i.e., three displacement vector and three micro-rotation vector. The micro-rotation vector $\boldsymbol{\omega}$, which is the sum of the material rotation vector $\boldsymbol{\theta}$ plus the particle relative rotation vector with respect to the material, is an independent quantity with no direct dependence upon $\boldsymbol{u}$, i.e. $\boldsymbol{\omega} \neq \boldsymbol{\theta}$, so that the relative rotation tensor $\boldsymbol{\alpha}$ is not equal zero, which is different from other existing theories.

We postulate that the strain energy density w depends only upon the strain tensor $\boldsymbol{\varepsilon}$ and the curvature tensor $\boldsymbol{\chi}$ (Chen and Wang, in press), i.e. the relative rotation tensor $\boldsymbol{\alpha}$ has no contributions to the strain energy density w. It follows

$$\tau_{ij} = \frac{\partial w}{\partial \alpha_{ij}} = 0 \tag{10}$$

where τ_{ij} is the anti-symmetric part of Cauchy stress and the work conjugate of the relative rotation tensor $\boldsymbol{\alpha}$. In the following sections, the symmetric part of Cauchy stress is called Cauchy stress directly.

The deviatoric part s_{ij} of Cauchy stress and deviatoric part m'_{ij} of couple stress are defined as the work conjugates of ε'_{ij}, χ'_{ij} respectively; σ_m and m_m are defined as the work conjugates of ε_m and χ_m respectively, giving

$$\delta w = s_{ij}\delta\varepsilon'_{ij} + m'_{ij}\delta\chi'_{ij} + \sigma_m\delta\varepsilon_m + m_m\delta\chi_m \tag{11}$$

where $s_{ij} \equiv \sigma_{ij} - (1/3)\delta_{ij}\sigma_{kk}$ and $m'_{ij} \equiv m_{ij} - (1/3)\delta_{ij}m_{kk}$.

Eq. (11) enables one to determine s_{ij}, m'_{ij}, σ_m and m_m in terms of the strain and curvature states of the solid as

$$s_{ij} = \frac{\partial w}{\partial\varepsilon'_{ij}}, \quad m'_{ij} = \frac{\partial w}{\partial\chi'_{ij}}, \quad \sigma_m = \frac{\partial w}{\partial\varepsilon_m}, \quad m_m = \frac{\partial w}{\partial\chi_m} \tag{12}$$

According to the work by Fleck and Hutchinson (1993) and Fleck et al. (1994), it is mathematically convenient to assume that the strain energy density w depends only upon the single scalar strain measure E_e, where

$$E_e^2 = \varepsilon_e^2 + l_{cs}^2\chi_e^2 \tag{13}$$

where l_{cs} is an intrinsic material length, which reflects the size effects of the rotation gradient on the material behaviors.

Σ_e is the work conjugate of E_e and defined by

$$\Sigma_e = \frac{\mathrm{d}w(E_e)}{\mathrm{d}E_e} \tag{14}$$

Then Eq. (12) can be written as

$$s_{ij} = \frac{2\Sigma_e}{3E_e}\varepsilon'_{ij}, \quad m'_{ij} = \frac{2\Sigma_e}{3E_e}l_{cs}^2\chi'_{ij}, \quad \sigma_m = K\varepsilon_m, \quad m_m = K_1 l_{cs}^2\chi_m \tag{15}$$

where

$$\Sigma_e = (\sigma_e^2 + l_{cs}^{-2}m_e^2)^{1/2} \tag{16}$$

and

$$\begin{cases} \sigma_e^2 = \frac{3}{2}s_{ij}s_{ij} & m_e^2 = \frac{3}{2}m'_{ij}m'_{ij} \\ \varepsilon_e^2 = \frac{2}{3}\varepsilon'_{ij}\varepsilon'_{ij} & \chi_e^2 = \frac{2}{3}\chi'_{ij}\chi'_{ij} \end{cases} \tag{17}$$

and K is the volumetric modulus and K_1 is called the bend-torsion volumetric modulus.

2.4. New hardening law

The hardening relationship in conventional plasticity theory can be expressed as following

$$\sigma_e = A(\varepsilon_e) = \frac{\mathrm{d}w(\varepsilon_e)}{\mathrm{d}\varepsilon_e} \tag{18}$$

and the incremental form of Eq. (18) is

$$\dot{\sigma}_e = A'(\varepsilon_e)\dot{\varepsilon}_e \tag{19}$$

where $A'(\varepsilon_e)$ is the tangent-hardening modulus in the incremental version of conventional J_2-deformation theory.

While the stretch gradient is not considered, the relation between Σ_e and E_e in this paper is taken as

$$\begin{cases} \Sigma_e = \Sigma_0 E_e^n, & \Sigma_e \geqslant \sigma_Y \\ \Sigma_e = 3\mu E_e, & \Sigma_e < \sigma_Y \end{cases} \tag{20}$$

While the stretch gradient is considered, the hardening strength is related with not only the density of statistically stored dislocation but also the density of geometrically necessary dislocation. Instructed by this idea, the new incremental hardening relationship similar to that in Chen and Wang (2000a) instead of Eq. (20) is proposed

$$\begin{cases} \dot{\Sigma}_e = A'(E_e)(1+\frac{l_1\eta_1}{E_e})^{1/2}\dot{E}_e = B(E_e, l_1\eta_1)\dot{E}_e & \Sigma_e \geqslant \sigma_Y \\ \dot{\Sigma}_e = 3\mu\dot{E}_e & \Sigma_e < \sigma_Y \end{cases} \tag{21}$$

where $A(E_e) = \Sigma_0 E_e^n$, $B(E_e, l_1\eta_1)$ is the hardening function including the effect of strain gradient; η_1 is the effective stretch gradient defined in Eq. (9). μ is the shear modulus and l_1 is the second intrinsic material length, which reflects the stretch gradient.

On each incremental step, both the effective strain ε_e and the effective stretch gradient η_1 can be obtained from the updated displacement fields; the effective rotation gradient χ_e can be obtained from the updated rotation fields. Hence η_1 is only a given parameter in Eq. (21) and it does not invoke higher-order stress or higher-order strain rates.

2.5. Incremental constitutive relation

According to Eq. (15), the constitutive relations of the deformation theory are

$$\sigma_{ij} = s_{ij} + \sigma_m\delta_{ij} = \frac{2\Sigma_e}{3E_e}\varepsilon'_{ij} + K\varepsilon_m\delta_{ij} \tag{22}$$

$$m_{ij} = m'_{ij} + m_m\delta_{ij} = \frac{2\Sigma_e}{3E_e}l_{cs}^2\chi'_{ij} + K_1 l_{cs}^2\chi_m\delta_{ij} \tag{23}$$

While the stretch gradient is considered, the new hardening law (21) is in the incremental form, which ensures that there is no higher-order stress or higher-order strain rate introduced. In order to solve the crack tip field using the new strain gradient theory and the new hardening law, the constitutive relations must be in the incremental form also. From Eqs. (22) and (23), we obtain

$$\begin{cases} \dot{\sigma}_{ij} = 2\mu\dot{\varepsilon}'_{ij} + K\dot{\varepsilon}_m\delta_{ij}, \\ \dot{m}_{ij} = 2\mu l_{cs}^2\dot{\chi}'_{ij} + K_1 l_{cs}^2\dot{\chi}_m\delta_{ij}, \end{cases} \quad \Sigma_e < \Sigma_0 \tag{24}$$

$$\begin{cases} \dot{\sigma}_{ij} = \frac{2\Sigma_e}{3E_e}\dot{\varepsilon}'_{ij} + \frac{2\dot{\Sigma}_e}{3E_e}\varepsilon'_{ij} - \frac{2\Sigma_e}{3E_e^2}\varepsilon'_{ij}\dot{E}_e + K\dot{\varepsilon}_m\delta_{ij}, \\ \dot{m}_{ij} = \frac{2\Sigma_e}{3E_e}l_{cs}^2\dot{\chi}'_{ij} + \frac{2\dot{\Sigma}_e}{3E_e}l_{cs}^2\dot{\chi}'_{ij} - \frac{2\Sigma_e}{3E_e^2}l_{cs}^2\chi'_{ij}\dot{E}_e + K_1 l_{cs}^2\dot{\chi}_m\delta_{ij}, \end{cases} \quad \Sigma_e \geqslant \Sigma_0 \tag{25}$$

3. Numerical formulation with strain gradient effects

In this section, the finite element formulations are presented for the strain gradient deformation theory. The principal of virtual work requires

$$\int_V (\sigma_{ij}\,\delta\varepsilon_{ij} + m_{ij}\,\delta\chi_{ij})\,\mathrm{d}V = \int_S (t_k\,\delta u_k + q_k\,\delta\omega_k)\,\mathrm{d}S \tag{26}$$

where V and S are the volume and surface of the material, respectively. The virtual strains $\delta\varepsilon_{ij}$ are related to the virtual displacements δu_k via Eq. (1) and $\delta\chi_{ij}$ are related to the virtual rotation vector $\delta\omega_k$. t_k is surface stress traction and q_k is surface torque traction.

The displacement field can be interpolated by the element shape functions N and the nodal displacements. Similarly, the micro-rotation field can be interpolated by the element shape functions N and the nodal rotation vectors. The strains and strain gradients can be obtained from kinematic relations Eqs. (1), (2) and (6). The stresses are then obtained via the constitutive law Eq. (22). The nodal displacements and rotation vectors have to be solved incrementally due to the new incremental hardening law, i.e. Eq. (21). Therefore, the nodal displacements and the rotation vectors are solved for each loading step by rewriting the principle of virtual work Eq. (26) about the current solution as

$$\begin{aligned}\int_V (\Delta s_{ij}\,\delta\varepsilon'_{ij} + \Delta\sigma_m\,\delta\varepsilon_{kk} + \Delta m'_{ij}\,\delta\chi'_{ij} + \Delta m_m\,\delta\chi_{kk})\,\mathrm{d}V - \int_S (\Delta t_k\,\delta u_k + \Delta q_k\,\delta\omega_k)\,\mathrm{d}S \\ = -\int_V (s_{ij}\,\delta\varepsilon'_{ij} + \sigma_m\,\delta\varepsilon_{kk} + m'_{ij}\,\delta\chi'_{ij} + m_m\,\delta\chi_{kk})\,\mathrm{d}V + \int_S (t_k\,\delta u_k + q_k\,\delta\omega_k)\,\mathrm{d}S \end{aligned} \tag{27}$$

where the superscript prime denotes the deviatoric quantities, Δ on the left-hand side stands for increments, whereas the right-hand side involves the current quantities.

3.1. The nodal degrees of freedom

Due to the independent parameter ω_i is introduced in addition to the displacement u_i in the present strain gradient theory, which is different from the theory proposed by Fleck and Hutchinson (1993), one node has six degrees of freedom. For a 2D plane case there are three degrees of freedom, i.e. u_{ix}, u_{iy} and ω_i. The displacement field and the rotation vector field can be obtained through the shape function and the nodal displacement and nodal rotation vectors, i.e.

$$u_x = \sum_{i=1}^{n} N_i u_{ix} \tag{28}$$

$$u_y = \sum_{i=1}^{n} N_i u_{iy} \tag{29}$$

$$\omega = \sum_{i=1}^{n} N_i \omega_i \tag{30}$$

3.2. The stiffness matrix $\boldsymbol{D}$

It is noted that this kind of strain gradient theory belongs to the non-linear elastic problem. While the current flow stress Σ_e is less than the yield stress σ_Y, i.e. the material is in the linear elastic state, the elastic $\boldsymbol{D}$ matrix is the same as the classical one. While the current flow stress Σ_e is larger than the yield stress σ_Y, $\boldsymbol{D}$ matrix is

$$\begin{cases} D_{11} = K + \frac{4\Sigma_e}{9E_e} + \frac{4}{81E_e^2}(2\varepsilon_{xx} - \varepsilon_{yy})^2 \left[A'(E_e)\left(1 + \frac{l_1\eta_1}{E_e}\right)^{1/2} - \frac{\Sigma_e}{E_e} \right] \\ D_{12} = K - \frac{2\Sigma_e}{9E_e} + \frac{4}{81E_e^2}(2\varepsilon_{xx} - \varepsilon_{yy})(2\varepsilon_{yy} - \varepsilon_{xx}) \left[A'(E_e)\left(1 + \frac{l_1\eta_1}{E_e}\right)^{1/2} - \frac{\Sigma_e}{E_e} \right] \\ D_{13} = \frac{2}{27E_e^2}(2\varepsilon_{xx} - \varepsilon_{yy})\gamma_{xy} \left[A'(E_e)\left(1 + \frac{l_1\eta_1}{E_e}\right)^{1/2} - \frac{\Sigma_e}{E_e} \right] \\ D_{14} = \frac{4l^2}{27E_e^2}(2\varepsilon_{xx} - \varepsilon_{yy})\chi_{zx} \left[A'(E_e)\left(1 + \frac{l_1\eta_1}{E_e}\right)^{1/2} - \frac{\Sigma_e}{E_e} \right] \\ D_{15} = \frac{4l^2}{27E_e^2}(2\varepsilon_{xx} - \varepsilon_{yy})\chi_{zy} \left[A'(E_e)\left(1 + \frac{l_1\eta_1}{E_e}\right)^{1/2} - \frac{\Sigma_e}{E_e} \right] \end{cases} \tag{31a}$$

$$\begin{cases} D_{22} = K + \frac{4\Sigma_e}{9E_e} + \frac{4}{81E_e^2}(2\varepsilon_{yy} - \varepsilon_{xx})^2 \left[A'(E_e)\left(1 + \frac{l_1\eta_1}{E_e}\right)^{1/2} - \frac{\Sigma_e}{E_e} \right] \\ D_{23} = \frac{2}{27E_e^2}(2\varepsilon_{yy} - \varepsilon_{xx})\gamma_{xy} \left[A'(E_e)\left(1 + \frac{l_1\eta_1}{E_e}\right)^{1/2} - \frac{\Sigma_e}{E_e} \right] \\ D_{24} = \frac{4l^2}{27E_e^2}(2\varepsilon_{yy} - \varepsilon_{xx})\chi_{zx} \left[A'(E_e)\left(1 + \frac{l_1\eta_1}{E_e}\right)^{1/2} - \frac{\Sigma_e}{E_e} \right] \\ D_{25} = \frac{4l^2}{27E_e^2}(2\varepsilon_{yy} - \varepsilon_{xx})\chi_{zy} \left[A'(E_e)\left(1 + \frac{l_1\eta_1}{E_e}\right)^{1/2} - \frac{\Sigma_e}{E_e} \right] \end{cases} \tag{31b}$$

$$\begin{cases} D_{33} = \frac{\Sigma_e}{3E_e} + \frac{\gamma_{xy}^2}{9E_e^2} \left[A'(E_e)\left(1 + \frac{l_1\eta_1}{E_e}\right)^{1/2} - \frac{\Sigma_e}{E_e} \right] \\ D_{34} = \frac{2l^2}{9E_e^2}\gamma_{xy}\chi_{zx} \left[A'(E_e)\left(1 + \frac{l_1\eta_1}{E_e}\right)^{1/2} - \frac{\Sigma_e}{E_e} \right] \\ D_{35} = \frac{2l^2}{9E_e^2}\gamma_{xy}\chi_{zy} \left[A'(E_e)\left(1 + \frac{l_1\eta_1}{E_e}\right)^{1/2} - \frac{\Sigma_e}{E_e} \right] \end{cases} \tag{31c}$$

$$\begin{cases} D_{44} = \frac{2l^2\Sigma_e}{3E_e} + \frac{4l^4}{9E_e^2}\chi_{zx}^2 \left[A'(E_e)\left(1 + \frac{l_1\eta_1}{E_e}\right)^{1/2} - \frac{\Sigma_e}{E_e} \right] \\ D_{45} = \frac{4l^4}{9E_e^2}\chi_{zx}\chi_{zy} \left[A'(E_e)\left(1 + \frac{l_1\eta_1}{E_e}\right)^{1/2} - \frac{\Sigma_e}{E_e} \right] \\ D_{55} = \frac{2l^2\Sigma_e}{3E_e} + \frac{4l^4}{9E_e^2}\chi_{zy}^2 \left[A'(E_e)\left(1 + \frac{l_1\eta_1}{E_e}\right)^{1/2} - \frac{\Sigma_e}{E_e} \right] \end{cases} \tag{31d}$$

where $l = l_{cs}$.

4. Finite element computation for crack tip fields

4.1. Choice of elements

Many researchers have found that the choice of element for gradient plasticity is complicated and in particular, quite sensitive to details of the constitutive relation. Xia and Hutchinson (1996) have discussed some choices of finite elements for strain gradient plasticity with the emphasis on plane strain cracks. Several elements have been developed for the phenomenological theory of strain gradient plasticity to

investigate the crack tip field, micro-indentation experiments and stress concentrations around a hole. A review of these elements can be found in the paper by Shu et al. (1999).

In order to consider the strain gradient, the constant strain element is excluded since there is no strain gradient in this kind of element. For the two-dimensional case, such as the problem of plane strain and the axis-symmetry, second-order element can be used, such as the eight-node and nine-node elements.

We have used two kinds of elements to study the plane strain crack tip fields. One is the eight-node isoparametric element and the other is the nine-node isoparametric element. Results for these two kinds of elements are almost the same so only the results for nine-node element are given below. The displacement and rotation vectors in the element are interpolated through the shape function, whereas the strain and the rotation gradient tensors in the element are then obtained via Eqs. (1) and (6). This element is only suitable for solids with vanishing higher-order stress traction on the surface. For example, the element has worked very well in the fracture analysis of strain gradient plasticity (Wei and Hutchinson, 1997; Chen et al., 1999), where the higher-order stress tractions vanish on the crack face and on the remote boundary. This element also works well in the study of micro-indentation experiments (Huang et al., 2000b) because the higher-order stress tractions are zero on the indented surface. Since the new strain gradient theory does not include higher-order stress and higher-order stress tractions, these kinds of elements will work well in the present study of plane strain crack tip field as discussed in the next section.

4.2. Computation model

The plane strain crack tip field is studied in the present paper. The domain for the finite element analysis is a circle, whose central point is at the crack tip and the radius is $R = 1000 l_{cs}$ as shown in Fig. 1, in which we take $R = 3000$ μm as the circle radius, i.e. the reference material parameter $l_{cs} = 3.0$ μm. It should be pointed out that the internal material length l_{cs} has been used to normalize r and K_{I} in the following text and does not appear explicitly in the non-dimensional stress distributions. Here $l_{cs} = 3.0$ μm is only a length related with the computation domain. The classical K fields are imposed on the outer boundary. For the small scale yielding configuration, only the upper half geometry is made discrete by the symmetry of the problem. A fine mesh is used near the crack tip, around which the smallest element size is on the order of $10^{-3} l_{cs}$, and effort is made to ensure elements having aspect ratio close to 1. The computation model is shown in Fig. 1. In the present paper, several kinds of size ratios of neighboring element are computed and

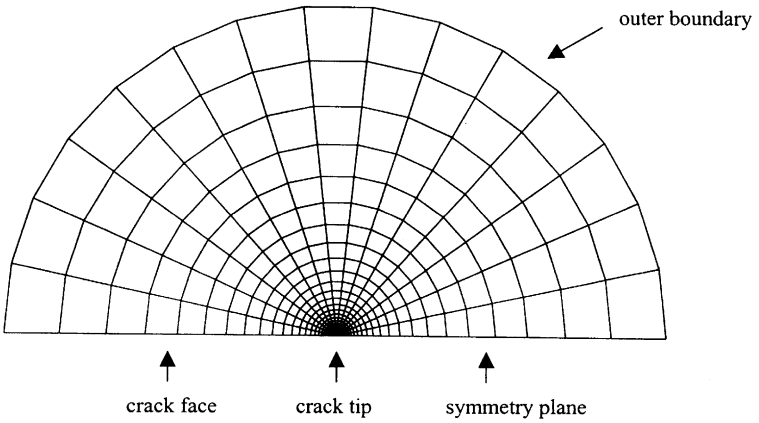

Fig. 1. Finite element mesh for crack tip problem using nine-node isoparametric element with $R = 1000 l_{cs}$.

it is found that the ratio has little influence on the calculating results. In the next section all the results are calculated adopting 1.2 of the neighboring element size ratio.

4.3. Boundary conditions

In the above section it is mentioned that the classical K field is imposed on the outer boundary and the detail normal and tangent stress tractions are as follows,

$$\begin{cases} \sigma_{rr} = \frac{K_I}{\sqrt{2\pi r}} \cos\frac{\theta}{2}\left(1 + \sin^2\frac{\theta}{2}\right) \\ \sigma_{r\theta} = \frac{K_I}{2\sqrt{2\pi r}} \cos\frac{\theta}{2}\sin\theta \end{cases} \tag{32}$$

where K_I is the stress intensity factor of mode I crack tip field. (r, θ) is the polar coordinate that the origin point is located at the crack tip.

The couple stress tractions on the outer boundary are taken as

$$m_{rr} = m_{\theta r} = 0 \tag{33}$$

On the boundary of the symmetric axis $(x > 0, y = 0)$, the displacement u_y, the micro-rotation ω_z and shear stress τ_{xy} are vanish.

On the crack surface, the stress tractions and the couple stress tractions are all vanish.

4.4. Numerical results

Numerical solutions obtained using the finite element methods are presented in this section. The nine-noded isoparametric element with three freedoms for each node is used and the mesh is shown in Fig. 1. The results presented below were computed with $\sigma_Y/E = 0.2\%$, $v = 0.3$, $R = 1000 l_{cs}$, although calculations were also carried out for other values of these parameters.

If the internal lengths l_{cs} and l_1 are zero, the strain gradient theory degenerates to be the classical theory. Fig. 2 shows the normalized effective stresses, σ_e/σ_Y, at polar angle $\theta = 0°$ versus the normalized distance r/l_{cs} ahead of the crack tip for the classical plasticity deformation theory (without strain gradient effects) and the plastic hardening exponent takes $n = 0.2$. Theoretical results of classical HRR solution and K field solution are shown in Fig. 2 also. The remotely applied stress intensity is $K_I/(\sigma_Y l_{cs}^{1/2}) = 20$. Here, it must be noted that during the finite element calculation we take $l_{cs} = l_1 = 0$ which means that no strain gradient effects are considered, l_{cs} in the normalized distance r/l_{cs} is not zero but the same as that used in the computation model, i.e. $l_{cs} = 3$ μm. While the curves of the theoretical results are drawn $l_{cs} = 3$ μm is also used to normalized the distance. From Fig. 2 we can find that the slope of near tip field is almost $-n/(n+1)$, which is consistent with the theoretical HRR field. Remote from the crack tip, the field tends to be K field with the slope to be $-1/2$. The calculation results are consistent with the theoretical results, which proves that the present calculation result (without strain gradient effects) is right.

In order to compare the results with those in Jiang et al. (2001), we first take the relation between the internal material lengths as $l_1 = l_{cs}$.

Fig. 3 shows the normalized effective stresses, σ_e/σ_Y at polar angle $\theta = 0°$ versus the normalized distance r/l_{cs} for the present strain gradient theory with the plastic hardening exponent $n = 0.2$ and $l_1 = l_{cs}$. The remotely applied stress intensity factor is $K_I/(\sigma_Y l_{cs}^{1/2}) = 20$. The plastic zone size is a bit more than $10 l_{cs}$, which is almost the same as that in Jiang et al. (2001) with the same stress intensity factor. The corresponding stress distribution in classical plasticity (without strain gradient effects) is also shown in Fig. 3. It is observed that, outside the plastic zone, both the present strain gradient theory and the classical plasticity theory give the same straight line with slope $-1/2$, which corresponds to the elastic K field. The predictions of the present strain gradient theory and the classical plasticity theory are almost the same within the plastic

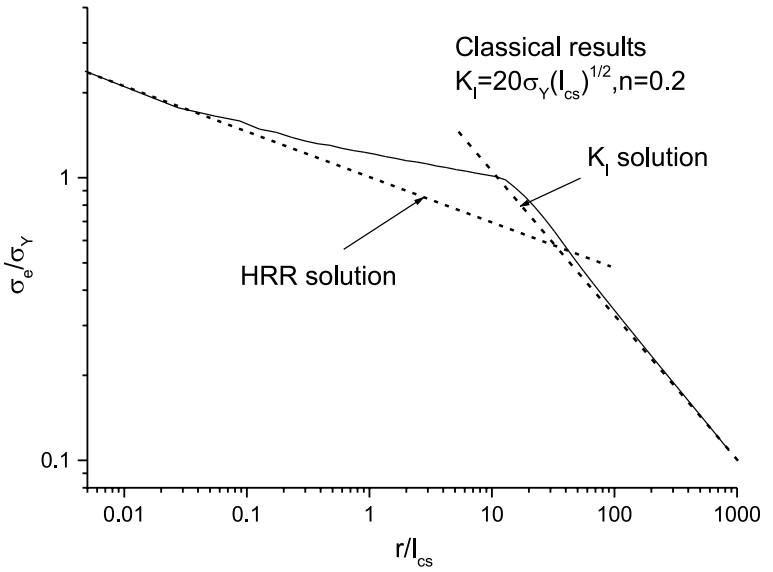

Fig. 2. Distributions of normalized effective stresses σ_e/σ_Y ahead of the crack tip at polar angle $\theta = 0°$ versus the normalized distance r/l_{cs} for the conventional plasticity deformation theory with external loading $K_I/(\sigma_Y l_{cs}^{1/2}) = 20$. Comparisons between the present calculation result and the theoretical results of HRR solution and K field solution are also shown.

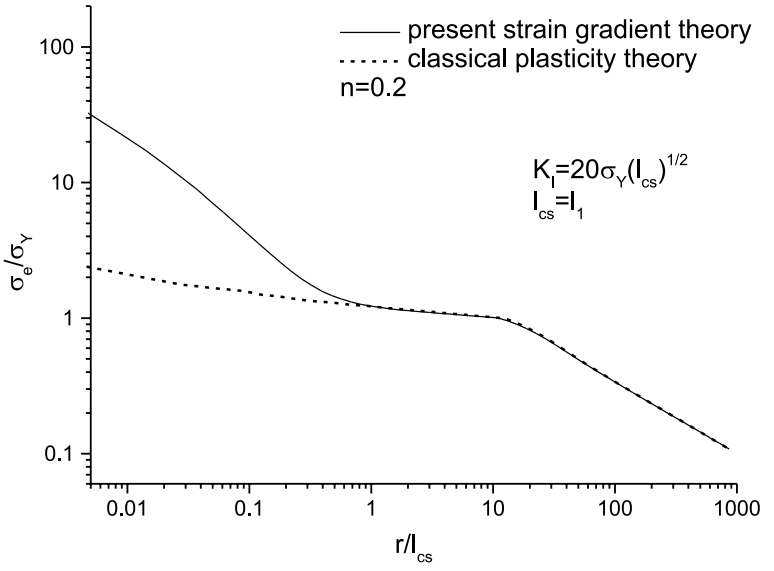

Fig. 3. Distributions of normalized effective stresses σ_e/σ_Y ahead of the crack tip at polar angle $\theta = 0°$ versus the normalized distance r/l_{cs} with the external loading $K_I/(\sigma_Y l_{cs}^{1/2}) = 20$ and $n = 0.2$, $l_1 = l_{cs}$ for the present strain gradient theory and the classical plasticity deformation theory.

zone at a distance larger than $0.3l_{cs}$ to the crack tip, which also agrees with the estimates in Jiang et al. (2001) and Xia and Hutchinson (1996). The physical reasonability can be found in Jiang et al. (2001). At a distance of $0.1l_{cs}$ to the crack tip, the effective stress given by the present strain gradient theory is much higher than that in classical plasticity and the absolute value of the slope is larger than that for the HRR

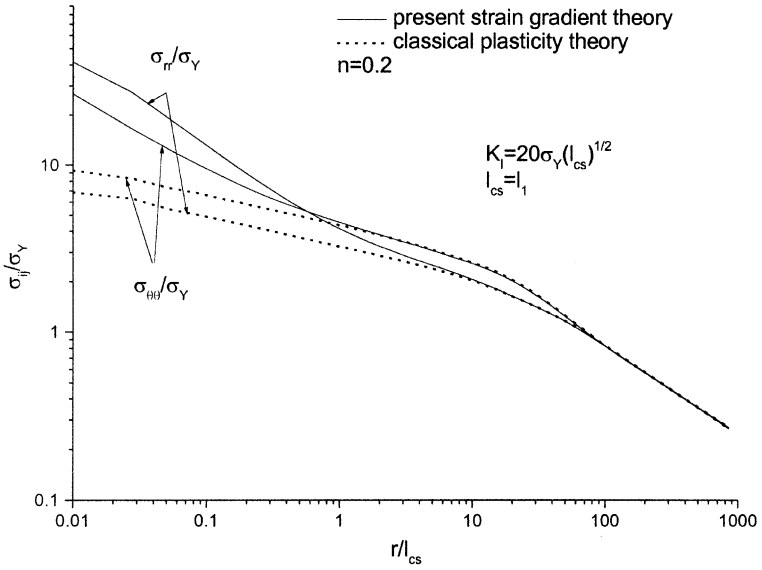

Fig. 4. Normalized stress components σ_{rr}/σ_Y, $\sigma_{\theta\theta}/\sigma_Y$ distributions versus the normalized distance r/l_{cs} with the external loading $K_I/(\sigma_Y l_{cs}^{1/2}) = 20$ and $n = 0.2$, $l_1 = l_{cs}$ for the present strain gradient theory and the classical plasticity theory.

field, which means that the stress singularity around the crack tip in the present strain gradient theory is stronger than that of the HRR field. The exponent of the stress singularity nearly tends to be $-1/2$. Similar results are obtained by Jiang et al. (2001). From Fig. 3 we can find that there is a strain gradient dominated zone near the crack tip, outside this kind of zone, it is a plasticity field and then K field.

The normalized stress components σ_{rr}/σ_Y and $\sigma_{\theta\theta}/\sigma_Y$ at polar angle $\theta = 0°$ versus the non-dimensional distance to the crack tip r/l_{cs} are shown in Fig. 4 for both the present strain gradient theory and the classical plasticity theory with the hardening exponent $n = 0.2$ and $l_1 = l_{cs}$. The remotely applied stress intensity factor is $K_I/(\sigma_Y l_{cs}^{1/2}) = 20$. The stress components around the crack tip predicted by the present theory and the classical plasticity theory are different within a distance of $0.1l_{cs}$ and the former is larger than the latter. From Fig. 4 we can find that the transition is clearly observed from the remote elastic K field to a plasticity field, then to the strain gradient dominated field.

According to Begley and Hutchinson (1997) and Stolken and Evans (1998), the relation between the intrinsic material lengths l_{cs} and l_1 basically is $l_1 \approx 0.1l_{cs}$.

Fig. 5 shows the normalized effective stresses, σ_e/σ_Y, at polar angle $\theta = 0°$ versus the normalized distance r/l_{cs} for the present strain gradient theory with the plastic hardening exponent $n = 0.2$ and $l_1 = 0.1l_{cs}$. The remotely applied stress intensity factor in Fig. 5 is $K_I/(\sigma_Y l_{cs}^{1/2}) = 20$. It must be noted that the relation between the intrinsic lengths l_1 and l_{cs} is different from that in Fig. 3. The plastic zone size is a bit more than $10l_{cs}$. The corresponding stress distribution in classical plasticity (without strain gradient effects) is also shown in Fig. 5. Outside the plastic zone, it is observed that both the present strain gradient theory and the classical plasticity theory give the same straight line with slope $-1/2$, which corresponds to the elastic K field. The predictions of the present strain gradient theory and the classical plasticity theory are almost the same within the plastic zone at a distance larger than $0.06l_{cs}$ to the crack tip. At a distance of $0.03l_{cs}$ to the crack tip, the effective stress given by the present strain gradient theory is much higher than that in classical plasticity and the absolute value of the slope is larger than that for the HRR field, which means that the stresses around the crack tip in the present strain gradient theory are more singular than the HRR field. The order of the stress singularity nearly tends to be $-1/2$. From Fig. 5 we can also find that there is a strain

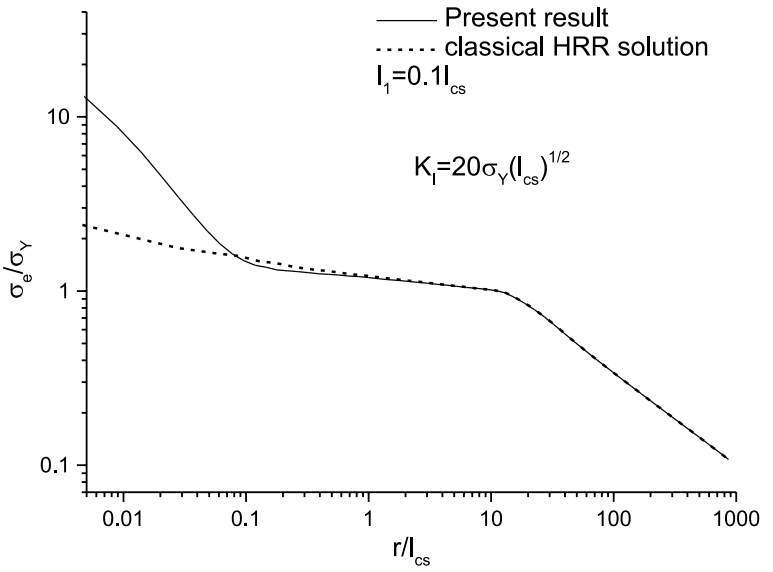

Fig. 5. Distributions of normalized effective stresses σ_e/σ_Y ahead of the crack tip at polar angle $\theta = 0°$ versus the normalized distance r/l_{cs} with the external loading $K_I/(\sigma_Y l_{cs}^{1/2}) = 20$ and $n = 0.2$, $l_1 = 0.1l_{cs}$ for the present strain gradient theory and the classical plasticity deformation theory.

gradient dominated zone near the crack tip, remote from the crack tip, it is a plasticity field and then K field dominates the outer field.

In Fig. 6, materials with various hardening exponents are calculated and the effects of the hardening exponents on the effective stress distribution ahead of the crack tip are shown in Fig. 6. The remotely

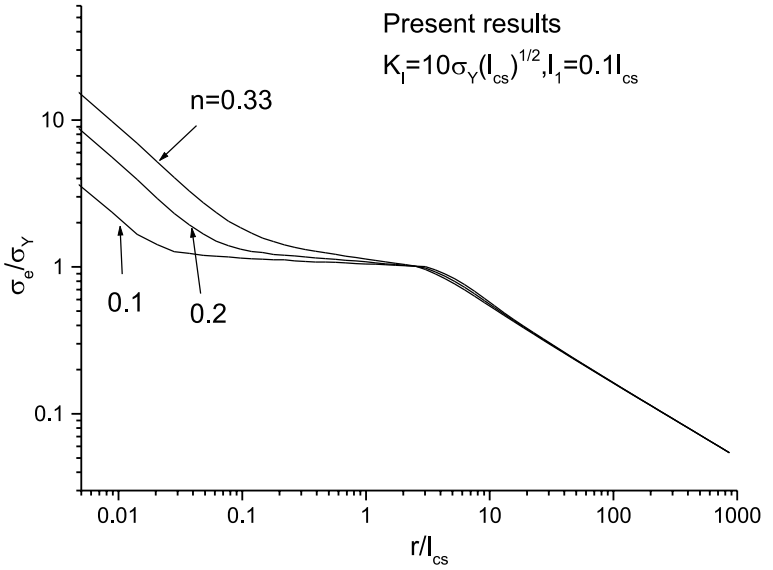

Fig. 6. Normalized effective stresses σ_e/σ_Y distributions versus the normalized distance r/l_{cs} for various hardening exponents with the external field $K_I/(\sigma_Y l_{cs}^{1/2}) = 10$ and $l_1 = 0.1l_{cs}$ for the present strain gradient theory.

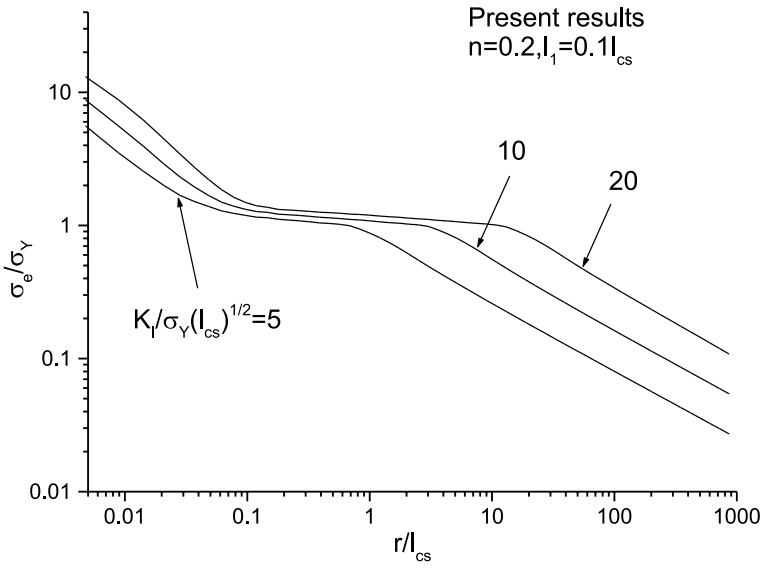

Fig. 7. Distribution of normalized effective stress σ_e/σ_Y versus the normalized distance r/l_{cs} for different loading: $K_{\mathrm{I}}/(\sigma_Y l_{cs}^{1/2}) = 5, 10, 20$. The hardening exponent is $n = 0.2$ and $l_1 = 0.1 l_{cs}$.

applied stress intensity factor is $K_{\mathrm{I}}/(\sigma_Y l_{cs}^{1/2}) = 10$ also and $l_1 = 0.1 l_{cs}$. The hardening exponents are $n = 0.1$, 0.2, 0.33. One can find from Fig. 6 that near the crack tip there is a domain dominated by the strain gradient, the slope is hardly related to the hardening exponents and nearly the same as that of classical K field. Remotely from the crack tip, there are a plastic field and classical K field. With the same remotely stress intensity factor and different hardening exponents, the plastic domain size is almost the same but with different slope, the classical K fields are the same and have no relation to the hardening exponents. The larger the hardening exponents, the higher the effective stress near the crack tip in the strain gradient dominated domain with the same external stress field.

Fig. 7 shows the normalized effective stress σ_e/σ_Y at polar angle $\theta = 0°$, versus the non-dimensional distance to the crack tip r/l_{cs} for four levels of remotely applied stress intensity factor, $K_{\mathrm{I}}/(\sigma_Y l_{cs}^{1/2}) = 5$, 10, 20 and the other parameters are identical. From Fig. 7, one can find that the size of the plastic zone increases quickly while the remotely applied stress intensity factor is increasing but the scale increase of near tip strain gradient dominated zone is not obvious and very slow, which shows that the strain gradient dominated zone is not sensitive to the outer K field and almost in the order of the intrinsic material length. From Fig. 7 it is easy to find that all curves approach to another set of straight lines, at the small distance to the crack tip, and the slope of the set of straight lines tends to be the same as that of classical K field. All these phenomena can be found also in Jiang et al. (2001), which analyzed the crack tip field with MSG theory (Gao et al., 1999).

Above calculation results seem to be consistent with the SSV model of Suo et al. (1993). The SSV model assumes that there is an elastic zone of height D above the interface in the metal film rightly near the interface crack tip. The size of height D is the same as the dislocation spacing. Plastic deformation occurs outside the elastic zone. The SSV model provides a reasonable picture for cleavage fracture in interface between a ductile metal film and thick oxide substrate.

The present calculation results confirm that the exponent of the stress singularity nearly tends to be $-1/2$, in despite of different plastic hardening exponents were simulated. It means that immediately near the crack tip, there is an elastic dominated zone.

5. Discussion

This paper presents a study of plane strain mode I crack tip field at micro-scale based on the new strain gradient theory. For remotely imposed classical K fields, the full field solutions are obtained numerically for elastic–plastic materials with strain gradient effects. It is found that the stresses near the crack tip are significant influenced by strain gradient effects. For mode I fracture under small scale yielding condition, transition from the remote classical K field to the near tip strain gradient dominated zone goes through a plasticity field. The singularity exponent in the strain gradient dominated domain is independent of the material plastic hardening exponents and is almost $-1/2$.

At a distance that is much larger than the dislocation spacing such that continuum plasticity is expected to be applicable. The near tip stresses predicted by the new strain gradient theory are significantly higher than that in HRR field. The increase in the near tip stress level provides an explanation to the experimental observation of cleavage fracture in ductile materials (Elssner et al., 1994).

While the relation of the two length scales is $l_1 = l_{cs}$, the numerical results are almost the same as that in Jiang et al. (2001), which proves that the new strain gradient seems to be capable of bridging the gap between the macroscopic cracking and atomic fracture also.

Acknowledgements

This work is supported by the National Natural Science Foundation of China (no. 19704100), National Science Foundation of Chinese Academy of Sciences (Project KJ951-1-20), CAS K. C. Wong Post-doctoral Research Award Fund and the Post-doctoral Science Fund of China.

References

Acharya, A., Bassani, J.L., 1995. On non-local flow theories that preserve the classical structure of incremental boundary value problems. In: Micromechanics of Plasticity and Damage of Multiphase Materials, IUTAM Symposium, Paris, August 29–September 1.

Acharya, A., Shawki, T.G., 1995. Thermodynamic restrictions on constitutive equations for second-deformation-gradient inelastic behavior. J. Mech. Phys. Solids 43, 1751–1772.

Aifantis, E.C., 1984. On the microstructural origin of certain inelastic models. Trans. ASME J. Eng. Mater. Technol. 106, 326–330.

Begley, M.R., Hutchinson, J.W., 1997. The mechanics of size-dependent indentation. J. Mech. Phys. Solids 46, 2049–2068.

Chen, J.Y., Huang, Y., Hwang, K.C., 1998. Mode I and mode II plane stress near tip fields for cracks in materials with strain gradient effects. Key Eng. Mater. 19, 145–149.

Chen, J.Y., Wei, Y., Huang, Y., Hutchinson, J.W., Hwang, K.C., 1999. The crack tip fields in strain gradient plasticity: the asymptotic and numerical analysis. Eng. Fract. Mech. 64, 2049–2068.

Chen, S.H., Wang, T.C., 2000a. A new hardening law for strain gradient plasticity. Acta Mater. 48, 3997–4005.

Chen, S.H., Wang, T.C., 2000b. Mode I crack tip field with strain gradient effects. Acta Mechanica Solida Sinica 13 (4), 290–298.

Chen, S.H., Wang, T.C., 2002. A new deformation theory for strain gradient effects. Int. J. Plast., 2002.

Chen, S.H., Wang, T.C., 2001. Mode I and mode II crack tip asymptotic fields with strain gradient effects. Acta Mechanica Sinica 17 (3), 269–280.

Elssner, G., Korn, D., Ruehle, M., 1994. The influence of interface impurities on fracture energy of UHV diffusion bonded metal-ceramic bicrystals. Scripta Metall. Mater. 31, 1037–1042.

Eringen, A.C., 1968. Theory of micropolar elasticity. In: Leibowitz, H. (Ed.), Fracture An Advanced Treatise. Academic Press, New York, pp. 621–729.

Fleck, N.A., Hutchinson, J.W., 1993. A phenomenological theory for strain gradient effects in plasticity. J. Mech. Phys. Solids 41, 1825–1857.

Fleck, N.A., Hutchinson, J.W., 1997. Strain gradient plasticity. In: Hutchinson, J.W., Wu, T.Y. (Eds.), Advances in Applied Mechanics, vol. 33. Academic Press, New York, pp. 295–361.

Fleck, N.A., Muller, G.M., Ashby, M.F., Hutchinson, J.W., 1994. Strain gradient plasticity: theory and experiment. Acta Metal. et Mater. 42, 475–487.

Gao, H., Huang, Y., Nix, W.D., Hutchinson, J.W., 1999. Mechanism-based strain gradient plasticity—I. Theory. J. Mech. Phys. Solids 47, 1239–1263.

Green, A.E., Mcinnis, B.C., Naghdi, P.M., 1968. Elastic–plastic continua with simple force dipole. Int. J. Eng. Sci. 6, 373–394.

Gurtin, M.E., 1965a. Thermodynamics and the possibility of spatial interaction in rigid heat conductors. Arch. Ration. Mech. Anal. 18, 335–342.

Gurtin, M.E., 1965b. Thermodynamics and the possibility of spatial interaction in elastic materials. Arch. Ration. Mech. Anal. 19, 339–352.

Huang, Y., Chen, J.Y., Guo, T.F., Zhang, L., Hwang, K.C., 1999. Analysis and numerical studies on mode I and mode II fracture in elastic–plastic materials with strain gradient effects. Int. J. Fract. 100, 1–27.

Huang, Y., Gao, H., Nix, W.D., Hutchinson, J.W., 2000a. Mechanism-based strain gradient plasticity—II. Analysis. J. Mech. Phys. Solids 48, 99–128.

Huang, Y., Xue, Z., Gao, H., Nix, W.D., Xia, Z.C., 2000b. A study of micro-indentation hardness tests by mechanism-based strain gradient plasticity. J. Mater. Res. 15, 1786–1796.

Huang, Y., Zhang, L., Guo, T.F., Hwang, K.C., 1995. Near-tip fields for cracks in materials with strain-gradient effects. In: Willis, J.R. (Ed.), Proceeding of IUTAM Symposium on Nonlinear Analysis of Fracture. Kluwer Academic Publishers, Cambridge, England, pp. 231–242.

Huang, Y., Zhang, L., Guo, T.F., Hwang, K.C., 1997. Mixed mode near-tip fields for cracks in materials with strain gradient effects. J. Mech. Phys. Solids 45, 439–465.

Hutchinson, J.W., 1997. Linking scales in fracture mechanics. In: Karihaloo, B.L., Mai, Y.W., Ripley, M.I., Ritchie, R.O. (Eds.), Advances in Fracture Research. Pergamon, Amsterdam, pp. 1–14.

Jiang, H., Huang, Y., Zhuang, Z., Hwang, K.C., 2001. Fracture in mechanism-based strain gradient plasticity. J. Mech. Phys. Solids 49, 979–993.

Lloyd, D.J., 1994. Particle reinforced aluminum and magnesium matrix composites. Int. Mater. Rev. 39, 1–23.

Ma, Q., Clarke, D.R., 1995. Size dependent hardness in silver single crystals. J. Mater. Res. 10, 853–863.

McElhaney, K.W., Vlassak, J.J., Nix, W.D., 1998. Determination of indenter tip geometry and indentation contact area for depth-sensing indentation experiments. J. Mater. Res. 13, 1300–1306.

Mindlin, R.D., 1963. Influence of couple-stress on stress concentrations. Exp. Mech. 3, 1–7.

Mindlin, R.D., 1964. Microstructure in linear elasticity. Arch. Ration. Mech. Abal. 16, 51–78.

Muhlhaus, H.B., Aifantis, E.C., 1991. The influence of microstructure-induced gradients on the localization of deformation in viscoplastic materials. Acta Mech. 89, 217–231.

Naghdi, P.M., Srinivasa, A.R., 1993a. A dynamical theory of structured solids. I basic developments. Philos. Trans. R. Soc. London, A 345, 425–458.

Naghdi, P.M., Srinivasa, A.R., 1993b. A dynamical theory of structured solids. II special constitutive equations and special cases of the theory. Philos. Trans. R. Soc. London, A 345, 459–476.

Naghdi, P.M., Srinivasa, A.R., 1994. Some general results in the theory of crystallographic slip. ZAMP 45, 687–732.

Nix, W.D., 1989. Mechanical properties of tin films. Metall. Trans. 20A, 2217–2245.

Poole, W.J., Ashby, M.F., Fleck, N.A., 1996. The role of strain gradients in grain size effect for polycrystals. J. Mech. Phys. Solids 44, 465–495.

Schaefer, H., 1967. Das Cosserat-Kontinuum. Z. Anew. Math. Mech. 47, 485–498.

Shi, M.X., Huang, Y., Gao, H., Hwang, K.C., 2000. Non-existence of separable crack tip field in mechanism-based strain gradient plasticity. Int. J. Solids Struct. 37, 5995–6010.

Shizawa, K., Zbib, H.M., 1999. A thermodynamical theory of gradient elastoplasticity with dislocation density tensor I: Fundamentals. Int. J. Plast. 15, 899–938.

Shu, J.Y., King, W.E., Fleck, N.A., 1999. Finite elements for materials with strain gradient effects. Int. J. Numer. Meth. Eng. 44, 373–391.

Smyshlyaev, V.P., Fleck, N.A., 1996. The role of strain gradients in the grain size effect for polycrystals. J. Mech. Phys. Solids 44, 465–495.

Stolken, J.S., Evans, A.G., 1998. A microbend test method for measuring the plasticity length scale. Acta Mater. 46, 5109–5115.

Suo, Z., Shih, C.F., Varias, A.G., 1993. A theory for cleavage cracking in the presence of plastic flow. Acta Metall. Mater. 41, 1551–1557.

Toupin, R., 1962. Elastic materials with couple-stresses. Arch. Ration. Mech. Anal. 11, 385–414.

Wei, Y., Hutchinson, J.W., 1997. Steady-state crack growth and work of fracture for solids characterized by strain gradient plasticity. J. Mech. Phys. Solids 45, 1253–1273.

Xia, Z.C., Hutchinson, J.W., 1996. Crack tip fields in strain gradient plasticity. J. Mech. Phys. Solids 44, 1621–1648.

Zbib, H., Aifantis, E.C., 1989. On the localization and postlocalization behavior of plastic deformation. Part I. On the initiation of shear bands; Part II. On the evolution and thickness of shear bands. Part III. On the structure and velocity of Portevin-Le Chatelier bands. Res. Mech. 23, 261–277, 279–292, 293–305.